Electronic Supplementary Information

Dramatic acceleration by visible-light and mechanism of AuPd@ZIF-8-catalyzed ammonia borane methanolysis for efficient hydrogen production

*Naixin Kang,[a] Ruofan Shen, [b] Baojun Li, [b] * Fangyu Fu,[c] Bruno Espuche, [d] Sergio Moya,[d] Lionel Salmon,[e] Jean-Luc Pozzo,[a] * Didier Astruc[a]**

[a] ISM, UMR CNRS Nº 5255, Univ. Bordeaux, 33405 Talence Cedex, France.

[b] Research Center of Green Catalysis, College of Chemistry, Zhengzhou University, 100 Science Road, Zhengzhou 450001, P. R. China.

[c] MOE Key Laboratory of Cluster Science, School of Chemistry and Chemical Engineering, Beijing Institute of Technology, Beijing 102488, P. R. China

[d] Soft Matter Nanotechnology Lab, CIC biomaGUNE, Paseo Miramón 182. 20014. Donostia-San Sebastián, Gipuzkoa, Spain.

[e] LCC, CNRS & University of Toulouse, 31077 Toulouse Cedex, France.

* Corresponding author: Didier Astruc, Baojun Li, Jean-Luc Pozzo

Email address: didier.astruc@u-bordeaux.fr, lbjfcl@zzu.edu.cn, jean-luc.pozzo@u-bordeaux.fr

Content

1. Materials and methods

-**Transmission Electron Microscopy (TEM)** and **high-resolution TEM (HRTEM)** were recorded using TEM JEOL JEM 1400 (120 kV)- 2100F.

-**Energy-dispersive X-ray Spectroscopy (EDS)** images were recorded using TEM-JEM-ARM200F Cold FEG equipped with a EDX spectrometer.

-**X-ray photoelectron spectra (XPS) System**: SPECS SAGE HR, X-Ray source: Mg Kα non-monochromatic, operated at 12.5 kV and 250 W. Take-off angle 90°, at ~10^{-8} Torr. Pass energy for survey spectra 30 eV, 15 eV for narrow scans. Analysis: spectra are calibrated to CC carbon 285 eV. Analysis consisted of Shirley background subtraction. Peaks are fitted with symmetrical Gaussian-Lorentzian (GL) line shapes. Samples were dispersed on a silica substrate, and its solvent was evaporated before measurement.

-**NMR spectra** were recorded at 25 °C with a Bruker AC 300, or 400 (300 or 400 MHz respectively). All the chemical shifts are reported in parts per million (δ, ppm) concerning Me_4Si for the ^1H NMR spectra

-**Inductively coupled plasma atomic emission spectroscopy (ICP-AES)**: Thermo Scientific iCAP 6300 DUO spectrometer with a 3-channel, 12-roller pump and a 27.12 MHz solid state RF plasma generator.

-**BET** areas were recorded with a 30% v/v N_2/He flow using pure N_2 (99.9%) as internal standard. At least 2 cycles of N_2 adsorption-desorption in the flow mode were employed to determine the total surface area using the standard single point method.

-**Finite-Difference-Time-Domain (FDTD**) calculations were performed by using Comsol Multiphysics 5.6 (COMSOL, Inc.) with perfectly matched layers (PML)

boundary conditions. For these simulations, a total-field scattered-field (TFSF) light source with wavelength ranges from 300 nm to 700 nm was used. The optical constant (n) of the AuPd@ZIF was determined according to the literature [1]. The size of the alloy and nanoparticle spacing were measured via TEM maps.

Synthesis of the ZIF-8 and ZIF-67

The method used for the preparation of ZIF-8 followed that reported previously [2]. Specifically, 2-methylimidazole (0.25 mol, 22.95 g) was dissolved in 250 mL methanol and stirred at room temperature to form a homogeneous solution. Then, an aqueous solution of $Zn(NO_3)_2 \cdot 6H_2O$ (13.7 g, 0.25 mol) dissolved in 250 mL methanol was rapidly injected into the above aqueous solution. The mixture was stirred for 8 h, and the product was collected by centrifugation and washed 3 times with water. The obtained solid was then dried at 60 °C *in vacuo* overnight, and the white solids were collected for further use. The synthesis method of ZIF-76 is the same as that for ZIF-8 upon replacement of $Zn(NO_3)_2 \cdot 6H_2O$ with $Co(NO_3)_2 \cdot 6H_2O$.

Synthesis of the UIO-66.

In a 250 mL Erlenmeyer flask, $ZrCl_4$ (334 mg) and CH_3COOH (7 mL) were completely dissolved in DMF (50 mL) under ultrasonic conditions. Then, *p*-phthalic acid (250 mg) dissolved in DMF (50 mL) was added to the aforementioned solution. The resulting mixture was sonicated for 10 min and kept at 120 °C for 24 h. After cooling to room temperature, the UIO-66 crystals were finally obtained by centrifugation and repeatedly washed with DMF [3].

H_2 detection. The reaction flask was connected by the gas outlet to a water-filled gas burette. When the gas was generated, the volume of gas evolved was determined periodically by measuring the displacement of water in the burette. In our two cases, 1 mmol AB produced 3 mmol H_2, corresponding to 67 mL H_2 at atmospheric pressure. Prior to the reactions, the volumes were measured at atmospheric pressure and

corrected for water vapor pressure at room temperature. Every reaction has been conducted three times, and the results are averaged.

NH_3 gas detection.

The gas generated from the methanolysis was passed through a 25 mL standard HCl solution (0.01 M) at room temperature, by which the ammonia gas was captured. After gas generation ceased, the resulting solution was titrated with standard NaOH solution (0.01 M) using the acid-base indicator phenolphthalein. The quantity of the liberated ammonia gas was calculated from the difference between two HCl solutions before and after the reaction.

TOF Calculation.

$TOF = mol_{H2\ released}/(total\ mol_{cat.} \times reaction\ time\ (min))$

TOF_s: the TOF value is related to the NP surface atoms number (Ns)

$V_{NP} = NV_{atom}$ (eq. 1)

$4/3\pi(R_{NP})^3 = N\ 4/3\pi(R_{atom})^3$ (eq. 2)

Where V is the atom volume of the NP, R is the atomic radius of the NP, and N is the total number of atoms within the NP. Rearranging, we obtain:

$N = (R_N P/R_{atom})^3$ (eq. 3)

Knowing the NP radius, we can also calculate the surface area (S) of a NP with the following equation:

$S_{NP} = 4\pi(R_{NP})^2$ (eq. 4)

So, we may also calculate the number of surface atoms (Ns) directly by dividing the surface area of the NP by the cross section of an individual NP atom and then simplifying using the relationship in (eq. 3):

$N_s = (4\pi(R_{NP})2) / (\pi\ (R_{atom})2) = 4\ N\ (R_{atom}/R_{NP})$ (eq. 5)

The ratio of the $N_s/N = 4\ (R_{atom}/R_{NP})$

So $TOF_s = TOF/(N_s/N)$

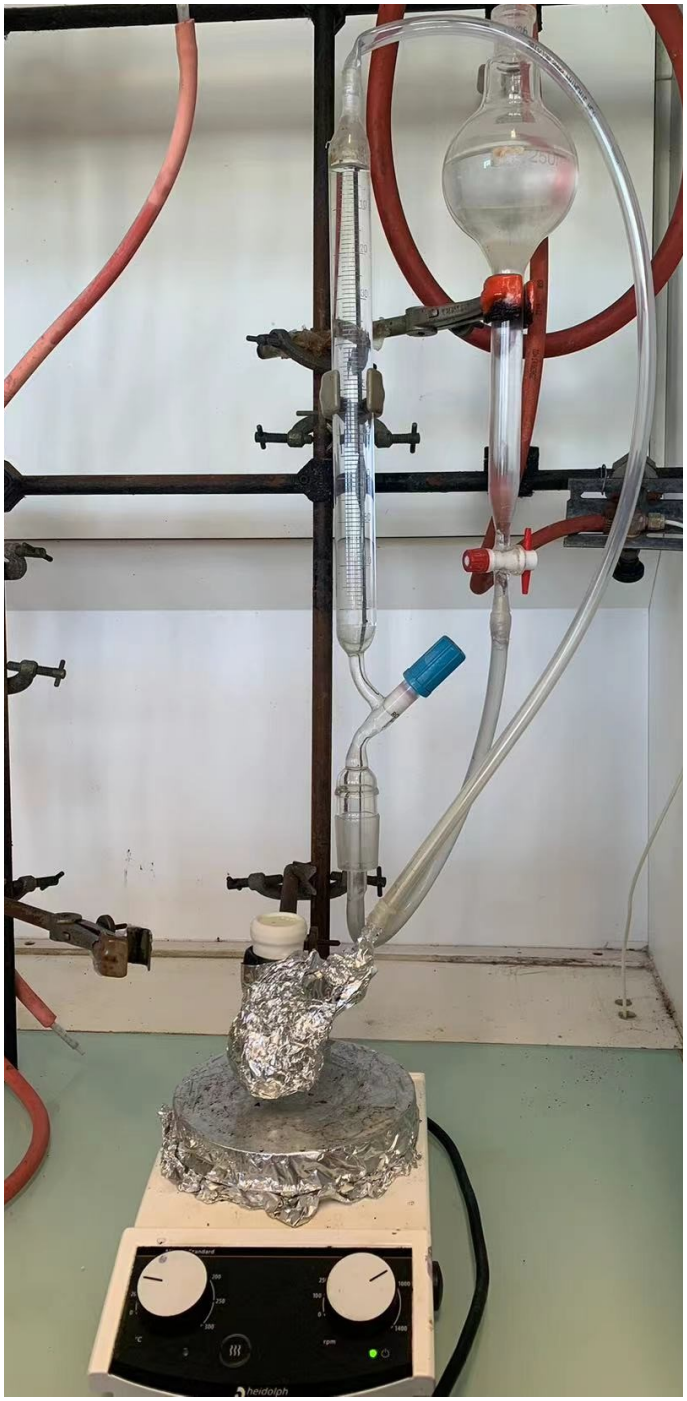

Fig. S1. The reaction for hydrogen generation from ammonia borane methanolysis in the dark.

Fig. S2. The raction for hydrogen generation from ammonia bornae methanolysis with visible light irradiation.

2. Characterization of the nanocatalysts

Table S1. Metal loading and atomic ratios of a series of catalysts measured by ICP-AES

Catalyst	Metal loading (wt%)	Atomic ratios
Au@ZIF-8	6.5	-
Pd@ZIF-8	4.2	-
$Au_{0.33}Pd_{0.67}$@ZIF-8	4.8	1:1.7
$Au_{0.25}Pd_{0.75}$@ZIF-8	4.5	1:2.6
$Au_{0.67}Pd_{0.33}$@ZIF-8	6.1	2.3:1
$Au_{0.5}Pd_{0.5}$@ZIF-8	5.7	1.1:1

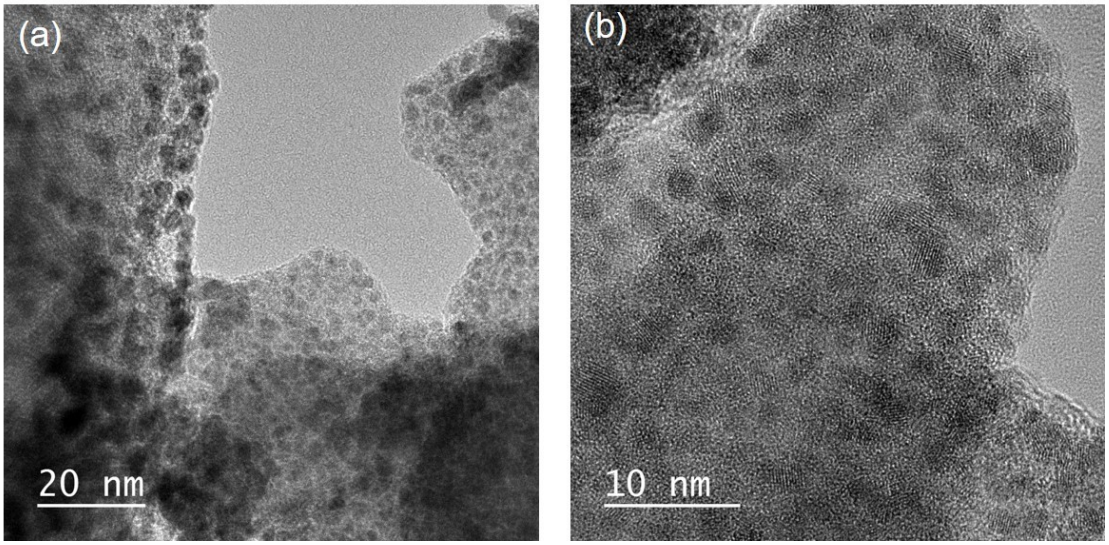

Fig. S3 (a) and (b) HRTEM images for AuPd@ZIF-8.

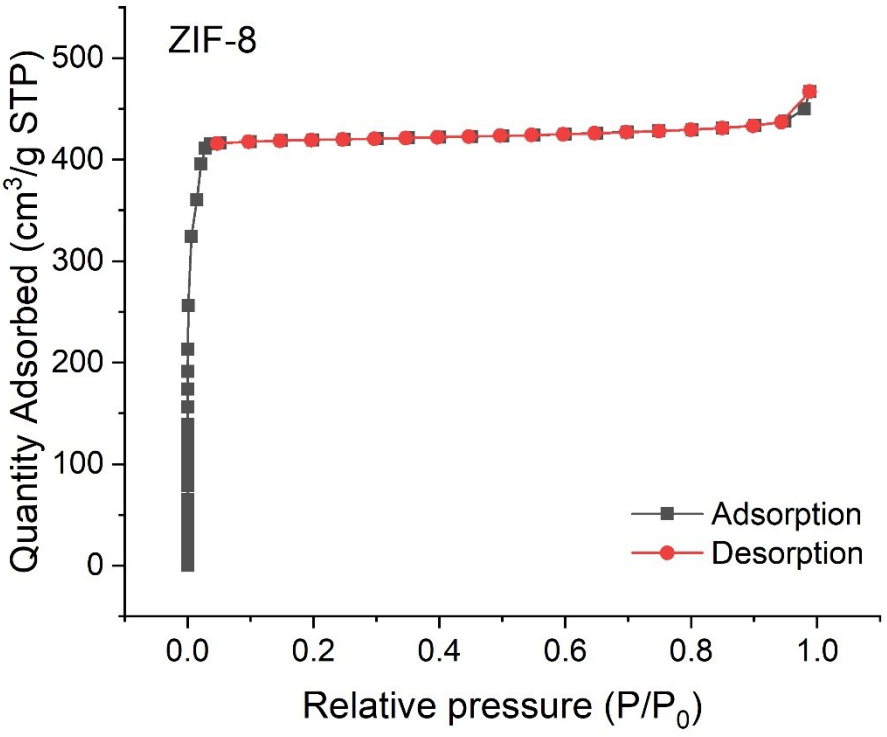

Fig. S4 Nitrogen adsorption-desorption isotherms of ZIF-8

Table S2. Physical properties of ZIF-8 and $Au_{0.5}Pd_{0.5}$@ZIF-8.

Sample	BET surface area ($m^2 \cdot g^{-1}$)	Pore width (nm)	Pore volume ($cm^3 \cdot g^{-1}$)
ZIF-8	1787.3	1.6	0.661
$Au_{0.5}Pd_{0.5}$@ZIF-8	1269.0	1.6	0.594

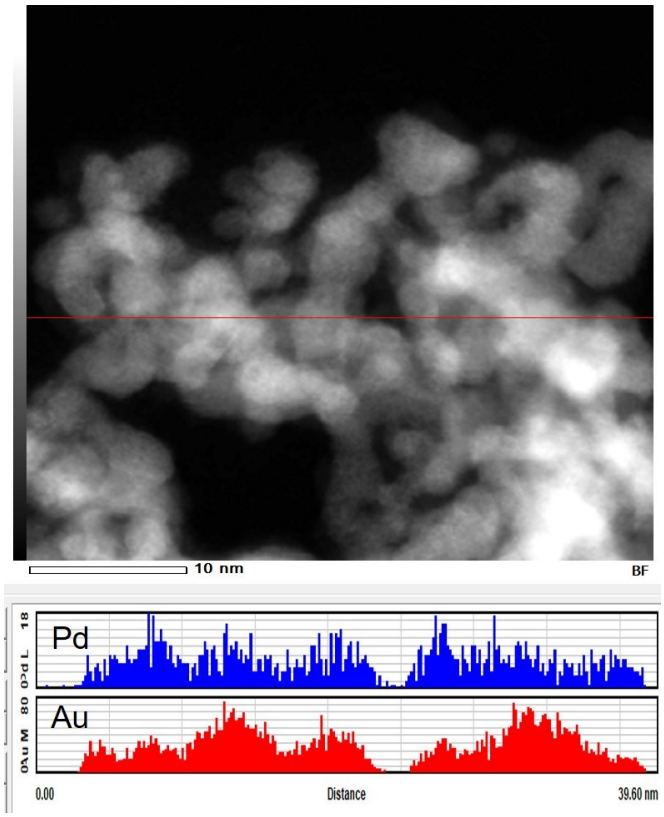

Fig. S5. HAADF-STEM image of AuPd@ZIF-8 and distributions of Au and Pd along cross-section lines.

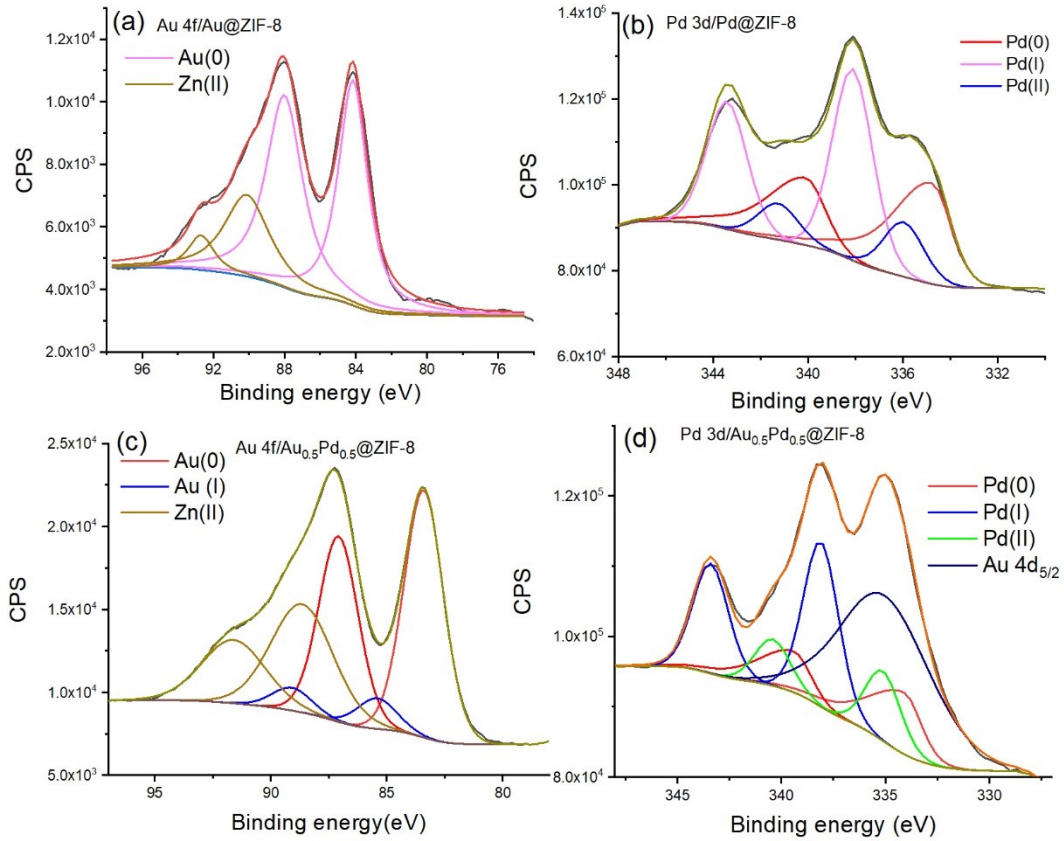

Fig. S6. (a) XPS spectra of Au@ZIF-8 in the Au 4f region, (b) XPS spectra of Pd@ZIF-8 in the Pd 3d region, (c) XPS spectra of $Au_{0.5}Pd_{0.5}$@ZIF-8 in the Au 4f region, (d) XPS spectra of $Au_{0.5}Pd_{0.5}$@ZIF-8 in the Pd 3d region.

Table S3. Binding energies of Au(0) and Pd(0) in Au 4f anf Pd 3d regions.

Samples	Au $4f_{7/2}$	Au $4f_{5/2}$	Pd $3d_{5/2}$	Pd $3d_{1/2}$
Au@ZIF-8	84.0	87.9	/	/
Pd@ZIF-8	/	/	334.9	340.2
$Au_{0.5}Pd_{0.5}$@ZIF-8	83.4	87.1	334.1	339.6

3. Methanolysis of ammonia borane

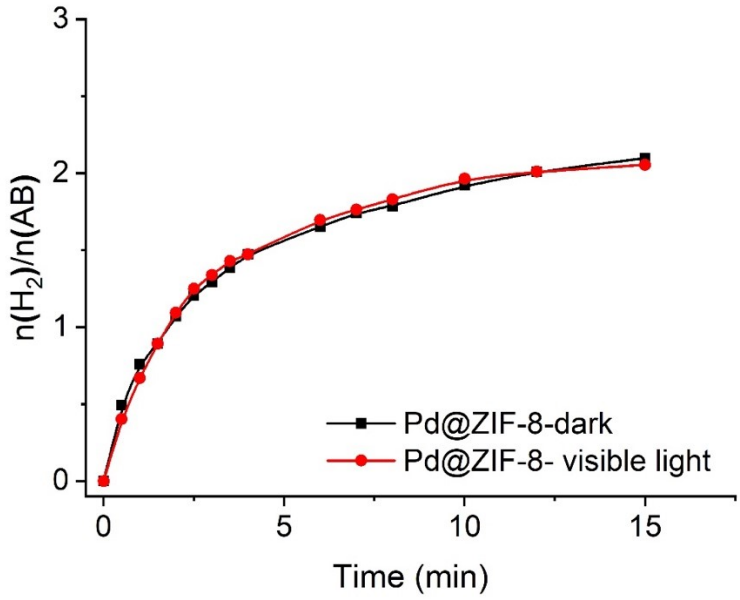

Fig. S7. Plot of the molar amount of H_2 generated upon AB methanolysis vs. time catalyzed by Pd@ZIF-8 with visible light and dark.

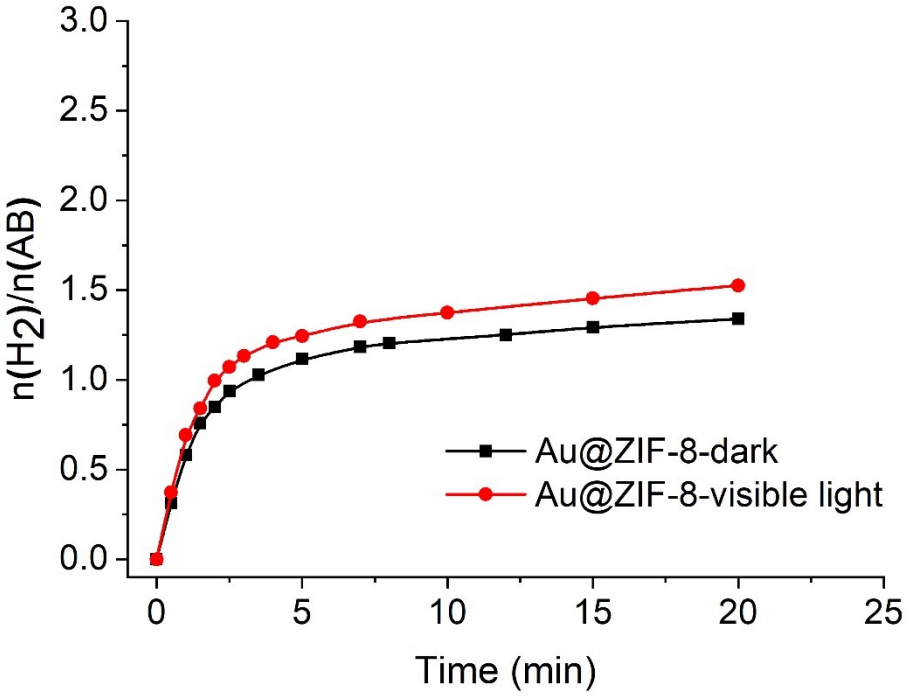

Fig. S8. Plot of the molar amount of H_2 generated upon AB methanolysis vs. time catalyzed by Au@ZIF-8 with visible light and dark.

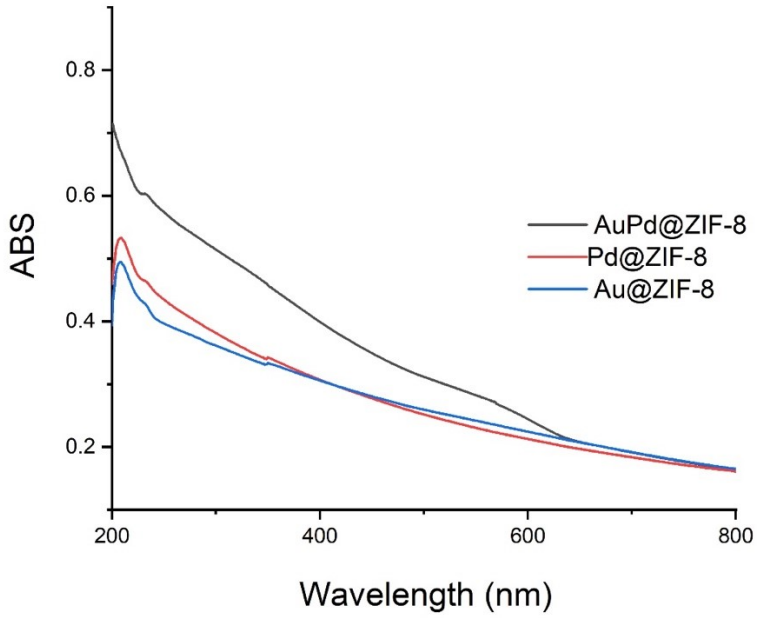

Fig. S9. UV-vis. spectra of Au@ZIF-8, $Au_{0.5}Pd_{0.5}$@ZIF-8, and Pd@ZIF-8.

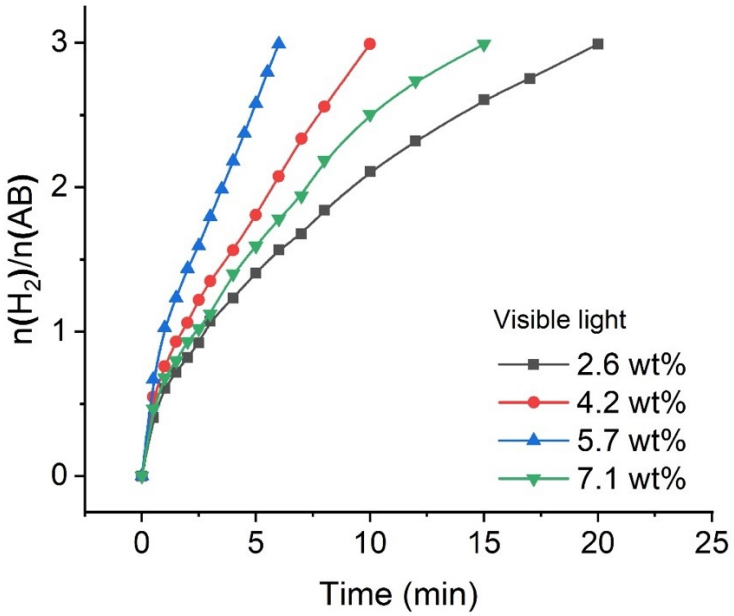

Fig. S10. Plot of molar amount of H_2 generated from AB methanolysis vs. time taken by different ZIF-8-stabilized Au-base bimetallic catalysts with different AuPd loading under visible light.

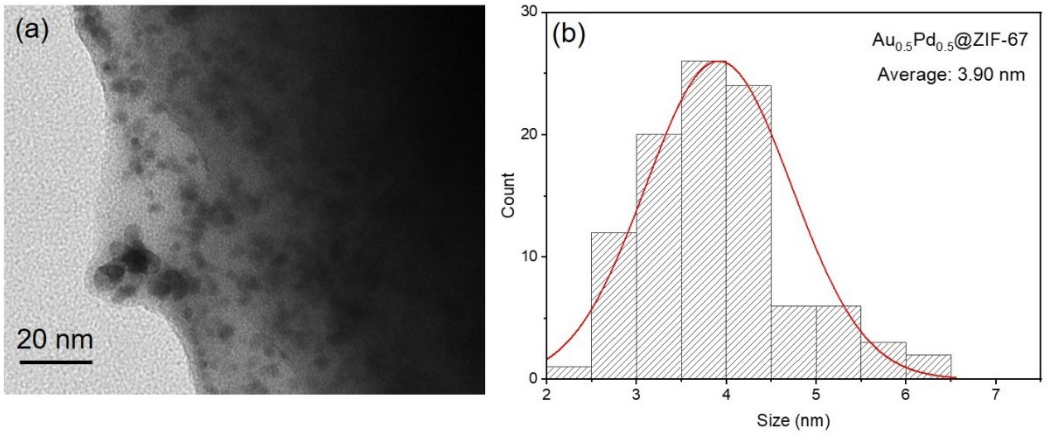

Fig. S11. (a) TEM image and (b) histogram of size distribution of the AuPd@ZIF-67.

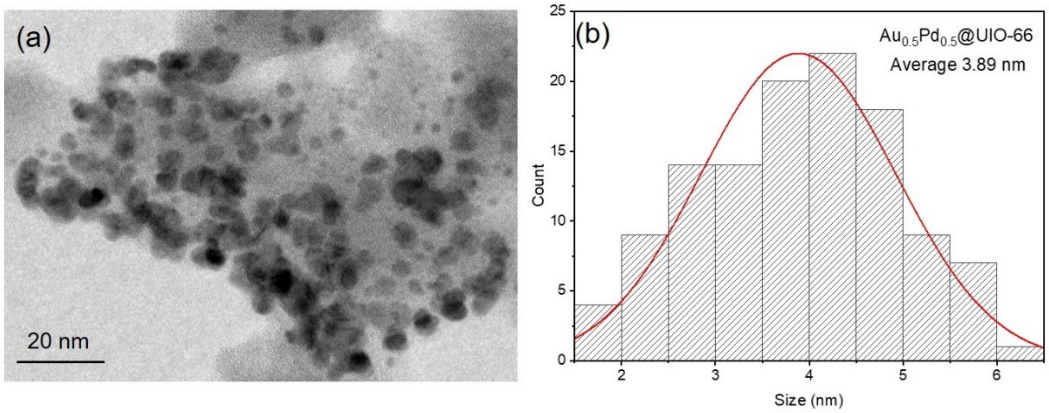

Fig. S12. (a) TEM image and (b) histogram of size distribution of the AuPd@UiO-66.

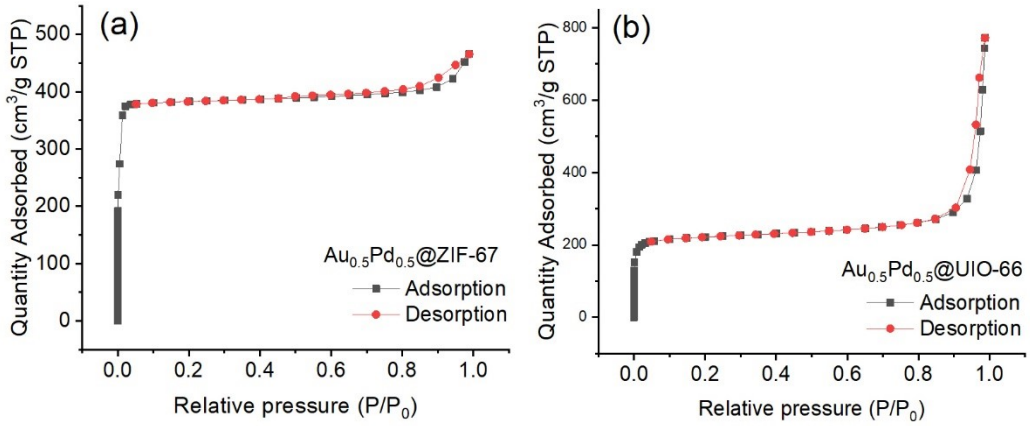

Fig. S13. Nitrogen adsorption-desorption isotherms of the AuPdNPs on different support (a) ZIF-67 and (b) UIO-66.

Table S4. Physical Properties of the AuPdNPs on ZIF-8, ZIF-67 and UIO-66.

Sample	BET surface area ($m^2 \cdot g^{-1}$)	Pore width (nm)	Pore volume ($cm^3 \cdot g^{-1}$)
$Au_{0.5}Pd_{0.5}$@ZIF-8	1269.0	1.6	0.594
$Au_{0.5}Pd_{0.5}$@ZIF-67	1511.3	1.7	0.671
$Au_{0.5}Pd_{0.5}$@UIO-66	877.0	5.4	0.780

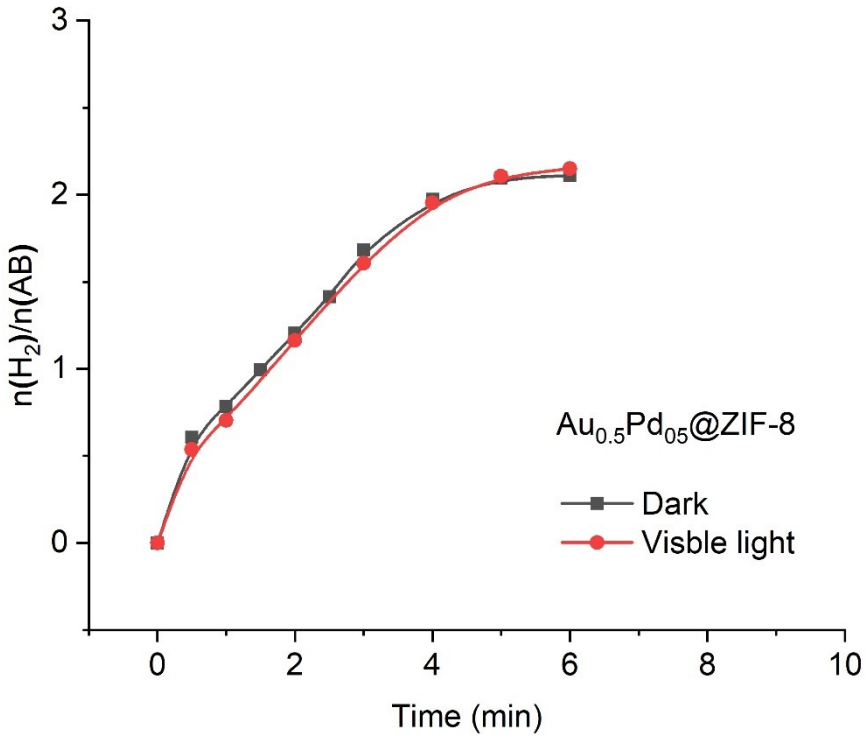

Fig. S14. AB methanolysis catalyzed by $Au_{0.5}Pd_{0.5}$@ZIF-8 in the dark and with visible light irradiation

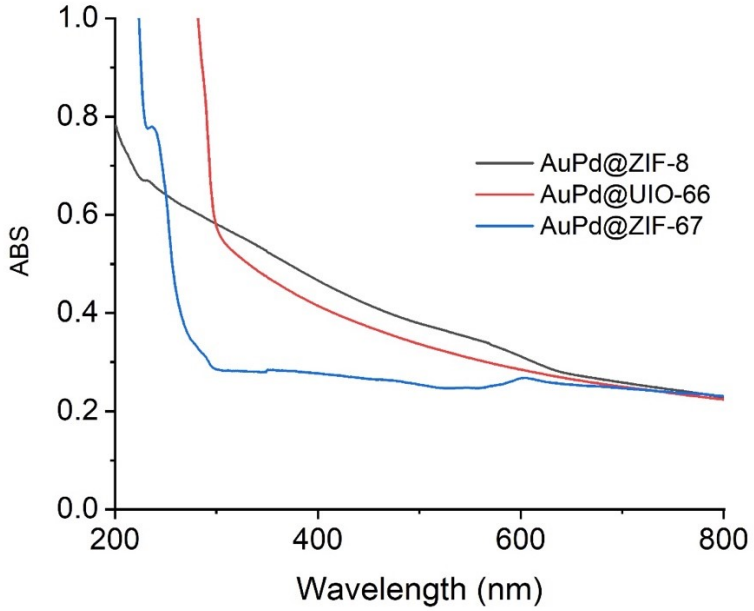

Fig. S15. UV-vis. spectra of $Au_{0.5}Pd_{0.5}$@ZIF-8, $Au_{0.5}Pd_{0.5}$@UIO-66 and $Au_{0.5}Pd_{0.5}$@ZIF-67.

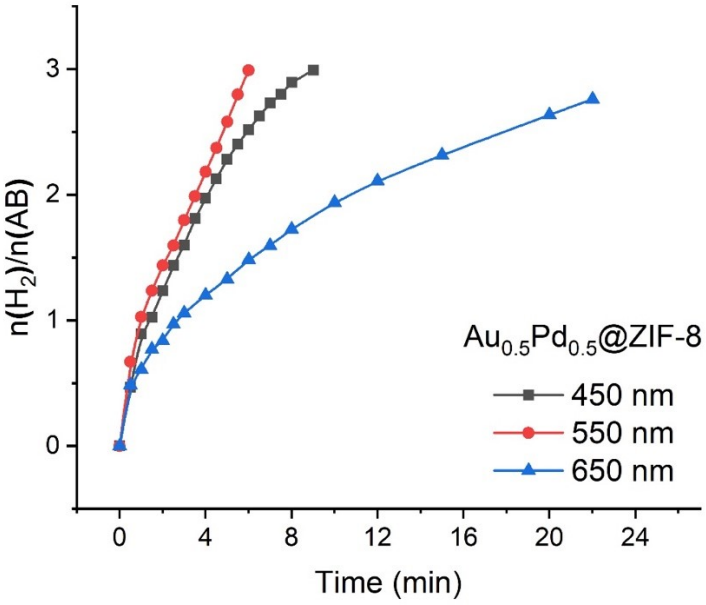

Fig. S16. AB methanolysis catalyzed by $Au_{0.5}Pd_{0.5}$@ZIF-8 under visible light irradiation with different wavelength.

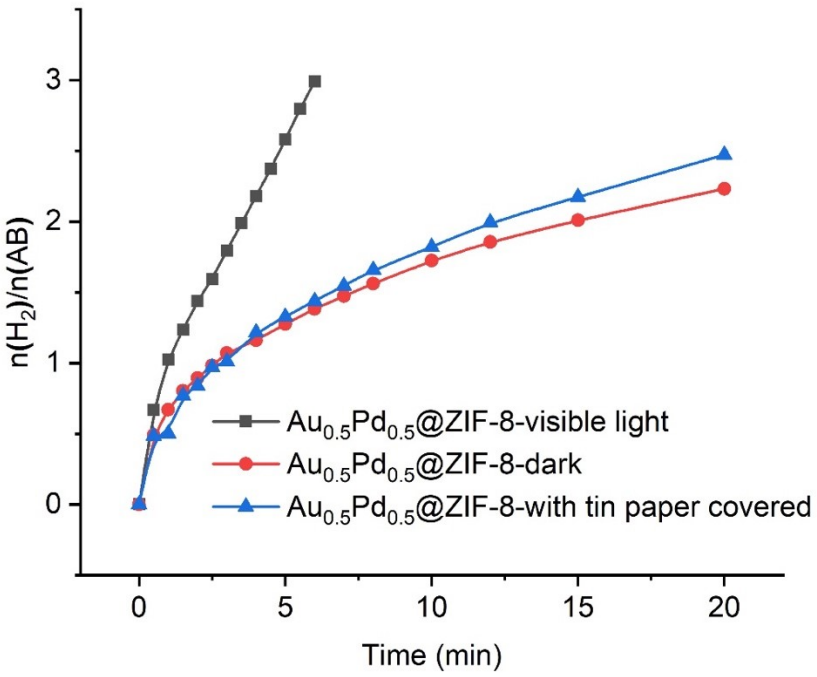

Fig. S17. Plot for molar amount of H_2 generated from AB methanolysis vs. time taken by AuPd@ZIF-8 under visible light irradiation, dark and tin paper covered.

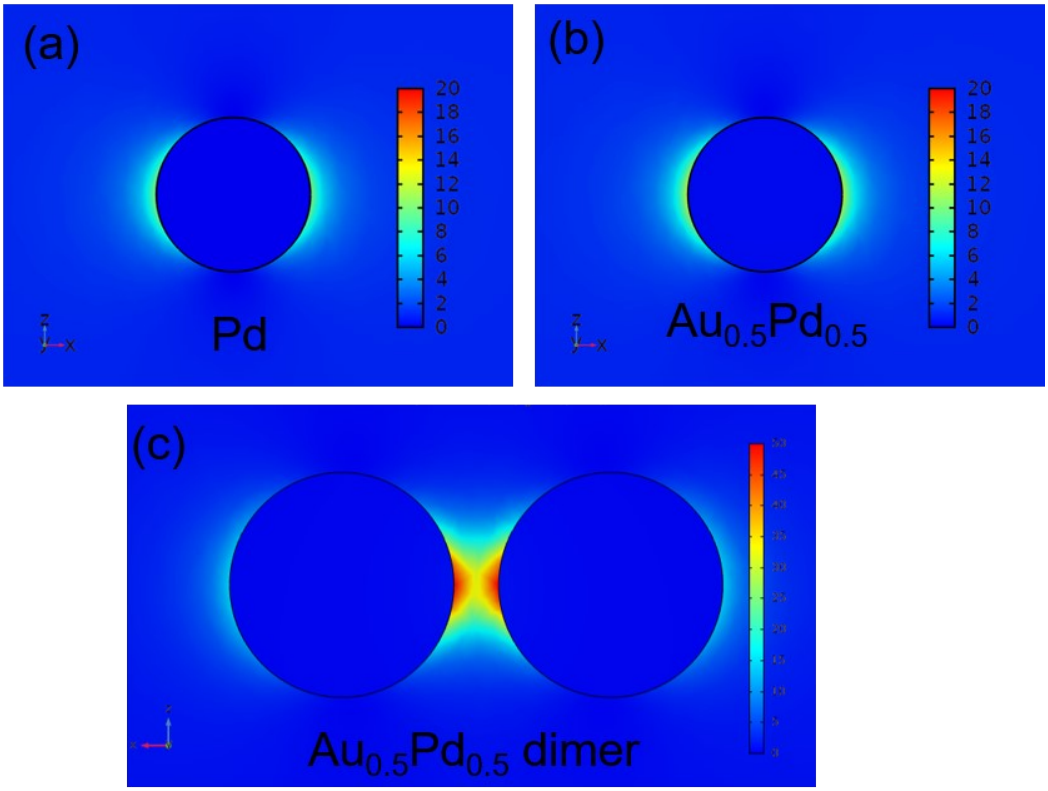

Fig. S18. Spatial distribution of the SPR-induced enhancement of electric field intensity from FDTD simulation calculated at the plasmon peak for (a) Pd (b) $Au_{0.5}Pd_{0.5}$ and $Au_{0.5}Pd_{0.5}$ dimer.

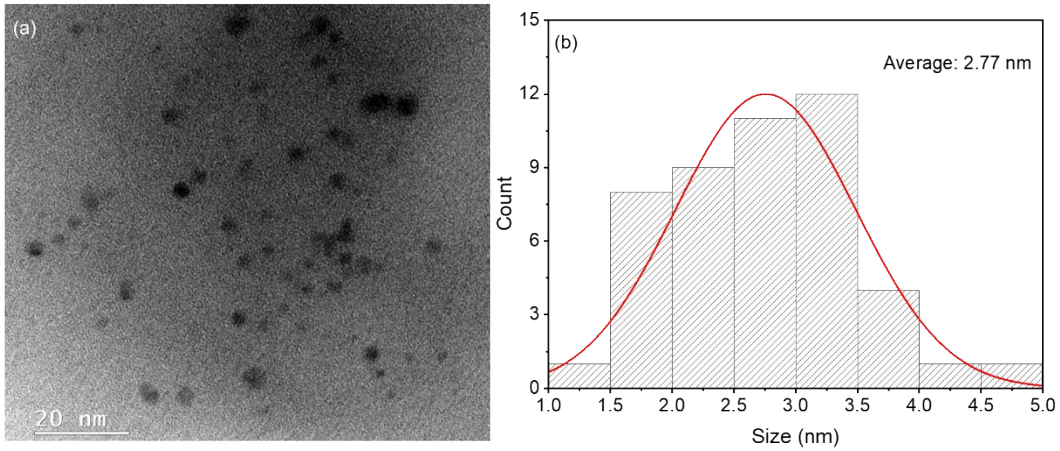

Fig. S19. (a) TEM image and (b) size distribution of the $Au_{0.5}Pd_{0.5}$@ZIF-8 after reaction.

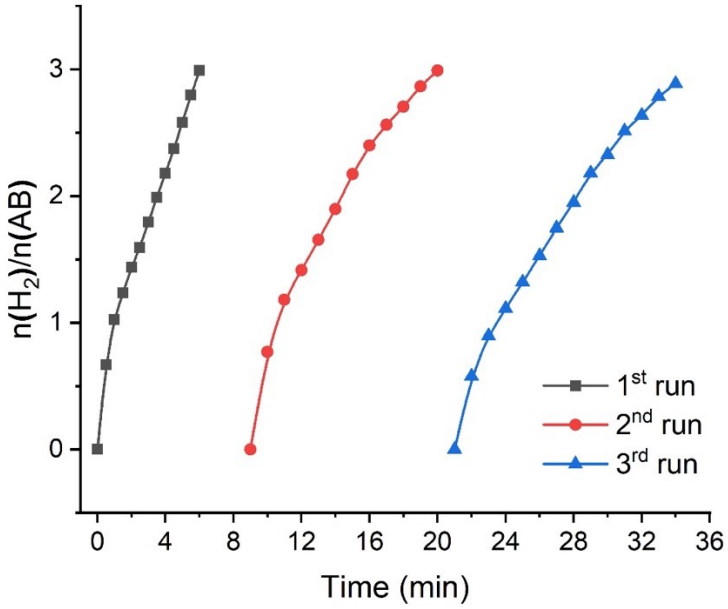

Fig. S20. Time plots of H_2 evolution for AB methanolysis catalyzed by $Au_{0.5}Pd_{0.5}$@ZIF-8 in the first, second, and third recycling tests with visible light irradiation.

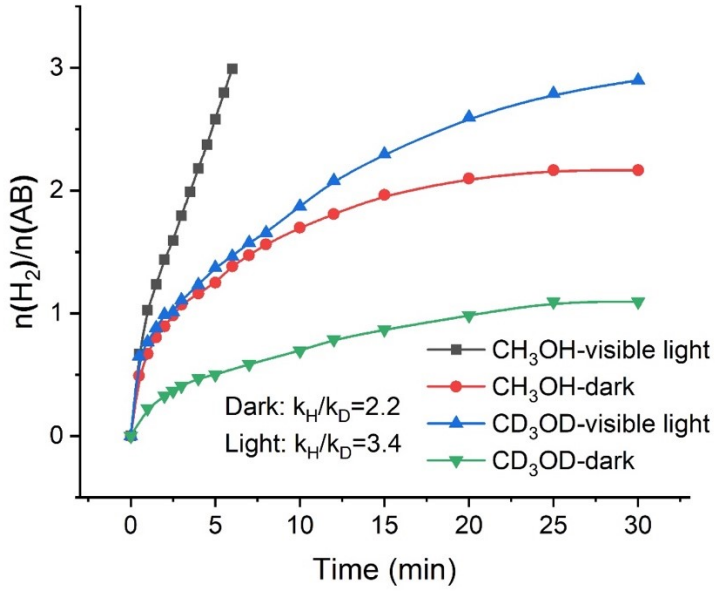

Fig. S21. Evolution of H_2 upon AB methanolysis with CH_3OH and CD_3OD catalyzed by $Au_{0.5}Pd_{0.5}$@ZIF-8 under visible light and dark.

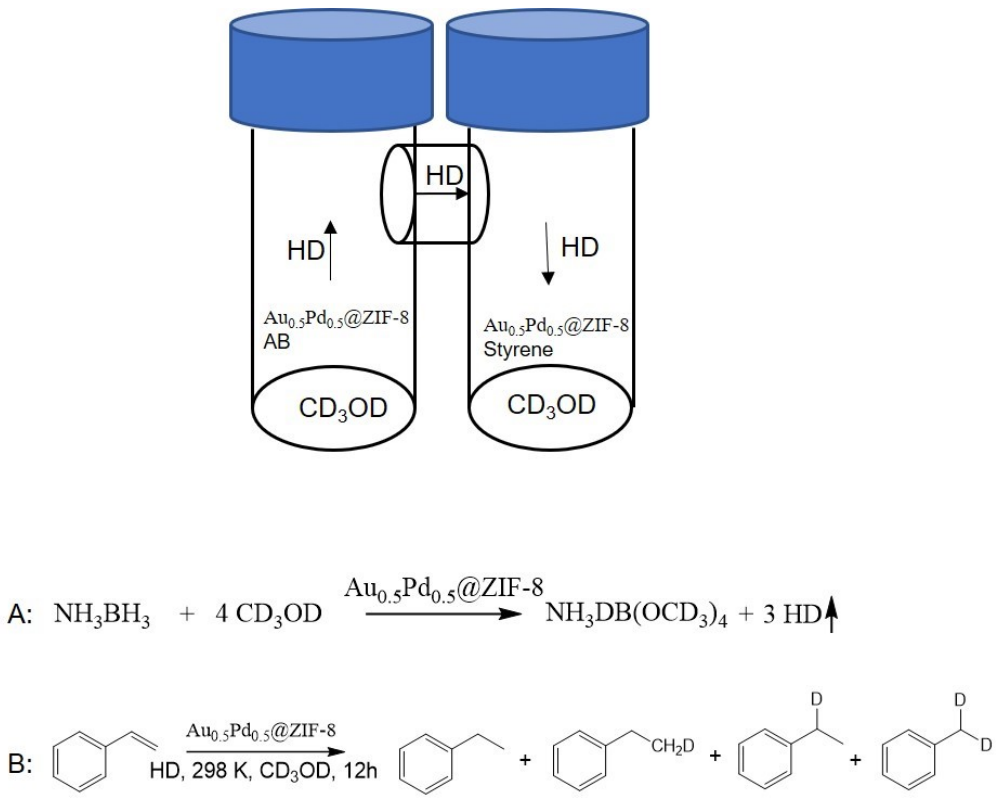

Fig. S22. Tandem reaction for the hydrogenation with "HD" generated from AB methanolysis catalyzed by $Au_{0.5}Pd_{0.5}$@ZIF-8.

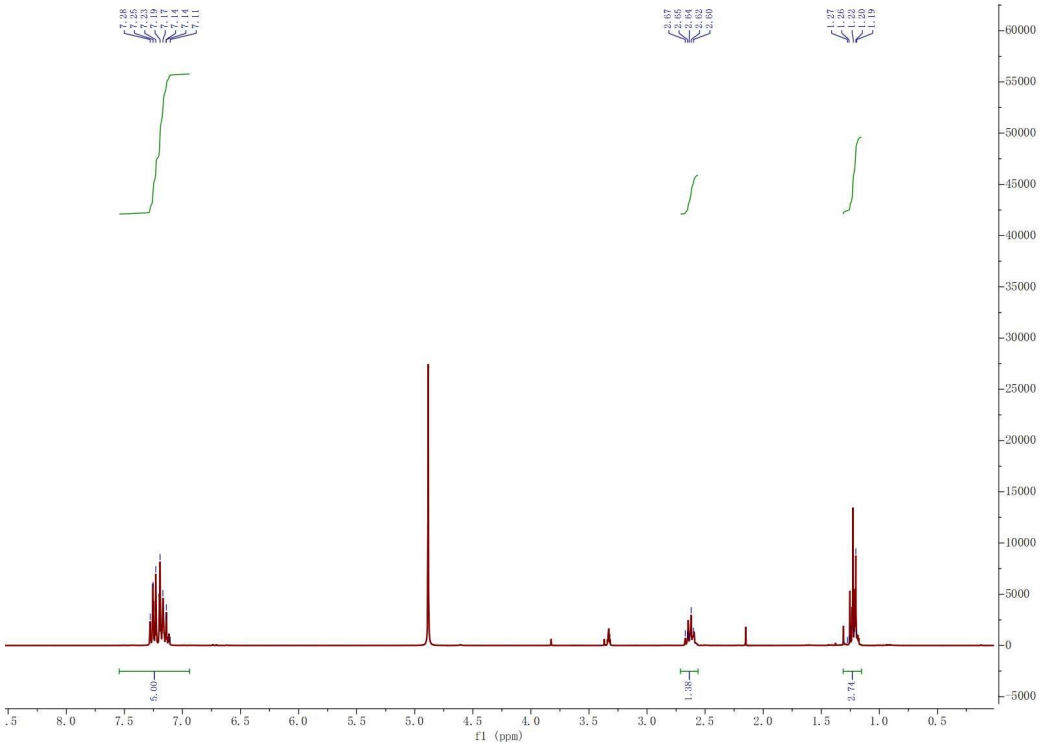

Fig. S23. ^{1}H NMR spectrum of ethylbenzene generated from the hydrogenation of styrene in tandem reaction ^{1}H NMR (300 MHz, CD_3OD), δ 7.31-7.12 (aromatic H, 5H), 2.67-2.60 (-CH_2, 1.38H), 1.27-1.19 (-CH_3, 2.74H).

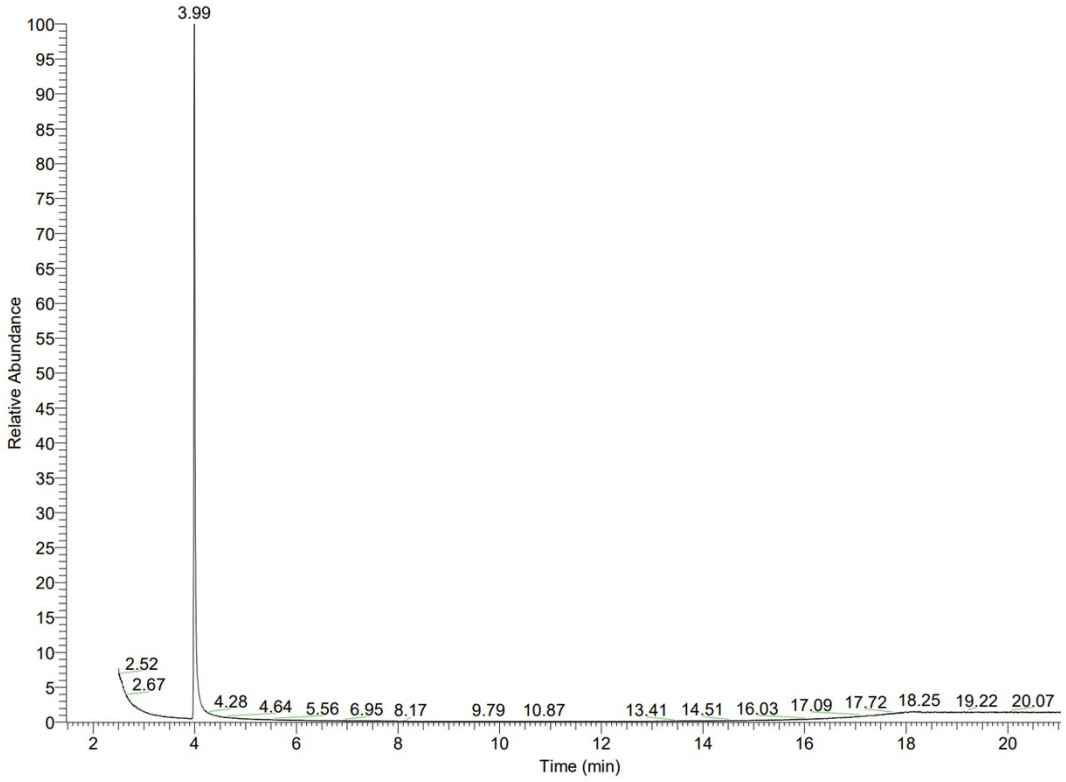

Fig. S24. GC-MS spectrum of the hydrogenation product of styrene.

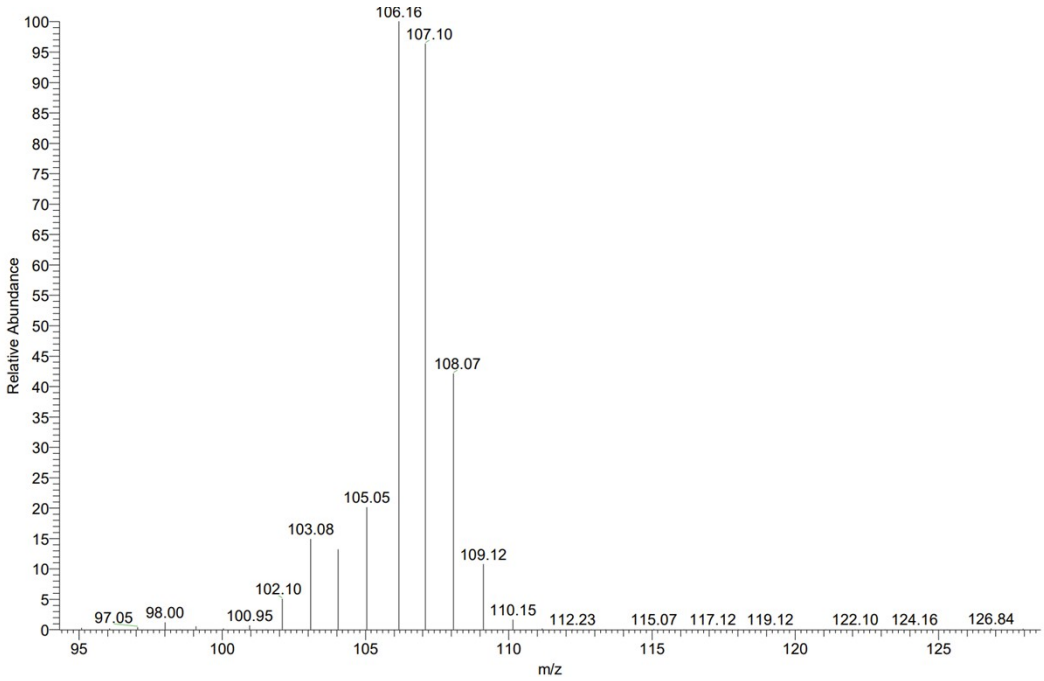

Fig. S25. MS spectrum at 3.99 min in Fig.S24 m/z 107.1 ($C_6H_5CHDCH_3$, $C_6H_5CHCH_2D$)

References

[1] S. Kadkhodazadeh, F.A.A. Nugroho, C. Langhammer, M. Beleggia, J.B. Wagner, Optical property–composition correlation in noble metal alloy nanoparticles studied with EELS, ACS Photonics. 6 (2019) 779–786.

[2] F.I. Pambudi, Electronic properties of heterometallic zeolitic imidazolate framework and its encapsulation with Ni , Pd and Pt, Inorg. Chem. Commun. 143 (2022) 109798. https://doi.org/10.1016/j.inoche.2022.109798.

[3] M.J. Katz, Z.J. Brown, Y.J. Colón, P.W. Siu, K.A. Scheidt, R.Q. Snurr, J.T. Hupp, O.K. Farha, A facile synthesis of UiO-66, UiO-67 and their derivatives, Chem. Commun. 49 (2013) 9449–9451.